CHEMISTRY OF MATERIALS
Article

Chem. Mater. **2009,** *21,* 3823–3829 3823
DOI:10.1021/cm901335k

Synthesis of Mesoporous Silica Nanoparticles via Controlled Hydrolysis and Condensation of Silicon Alkoxide

Zhen-An Qiao, Ling Zhang, Mingyi Guo, Yunling Liu, and Qisheng Huo*

State Key Laboratory of Inorganic Synthesis and Preparative Chemistry, College of Chemistry, Jilin University, Changchun 130012, China

Received May 14, 2009. Revised Manuscript Received July 5, 2009

The cooperative self-assembly of silica species and cationic surfactant cetyltrimethylammonium chloride (CTA^+Cl^- or CTAC) and the formation of mesoporous silica nanoparticles occur following the hydrolysis and condensation of silica precursor TEOS in the solution. The particle size can be controlled from ~25 nm to ~200 nm by adding suitable additive agents (e.g., inorganic bases, alcohols) which affect the hydrolysis and condensation of silica species. The in situ pH measurement of synthesis system is introduced to investigate the formation process of mesoporous silica nanoparticles. Our results show that a certain acid−base buffer capacity of the reaction mixture in a range of pH 6−10 is essential for the formation of mesoporous silica nanoparticles in the TEOS−CTA^+ system. The nucleation and growth process of the nanoparticles can be extended into the self-assembly system of inorganic−surfactant and the formation of mesophase in aqueous media.

Introduction

Since the discovery of M41S, mesoporous materials[1] have received particular attention in many areas, such as catalysis, adsorption, separation, chromatography, chemical sensors, and bioscience.[2] Monodisperse colloidal mesoporous silica nanoparticles have more potential for the above applications because of their nano-scaled size, in particular for a variety of nanotechnological applications including biomedicine and biotechnology.

Many research groups have reported various mesoporous silica particles from hundreds of nanometers to tens of micrometers.[3−11] For example, Unger et al.[12] synthesized aggregated 10−100 μm mesoporous particles which consisted of 50−100 nm primary particles. Park et al.[13] used microwave synthesis to get size changing from ~200 nm rounded particles to 1−2 μm wormlike structures by adding ethylene glycol. Imai et al.[6] successfully prepared nano-scaled particles with a diameter of 20−50 nm. Some groups obtained uniform and highly ordered mesoporous silica nanoparticles by using highly diluting methods, in which diluted surfactant concentration was used to overcome the particle aggregation.[14−18] However, it was very difficult to isolate the product, and the high dilution technique often resulted in low yields. Yano reported the synthesis of monodisperse mesoporous silica spheres from ~150 nm to ~900 nm by using conventional alkyltrimethylammonium halide as a surfactant.[10,11] Bein et al.[19−21] reported a high-yield synthesis procedure to synthesize the suspensions of colloidal mesoporous silica with 50−100 nm particle size by addition of triethanolamine (TEA). TEA was thought to act as a complexing agent for silicate species and additionally as an encapsulator for mesoporous particles, limiting the growth and aggregation of particles.

Although the formation of nano-scaled colloidal particles was achieved in many preparations, the key synthesis parameters are still in doubt. On the other hand, most mechanism work of mesoporous materials (e.g., MCM-41) formation so far has been done to illuminate the interaction

---

*Corresponding author. E-mail: huoqisheng@jlu.edu.cn.

(1) Beck, J. S.; Vartuli, J. C.; Roth, W. J.; Leonowicz, M. E.; Kresge, C. T.; Schmitt, K. D.; Chu, C. T. W.; Olson, D. H.; Sheppard, E. W. *J. Am. Chem. Soc.* **1992**, *114*(27), 10834–10843.
(2) Wan, Y.; Zhao, D. Y. *Chem. Rev.* **2007**, *107*(7), 2821–2860.
(3) Pauly, T. R.; Liu, Y.; Pinnavaia, T. J.; Billinge, S. J. L.; Rieker, T. P. *J. Am. Chem. Soc.* **1999**, *121*(38), 8835–8842.
(4) Pauwels, B.; Van Tendeloo, G.; Thoelen, C.; Van Rhijn, W.; Jacobs, P. A. *Adv. Mater.* **2001**, *13*(17), 1317–1320.
(5) Walcarius, A.; Delacote, C. *Chem. Mater.* **2003**, *15*(22), 4181–4192.
(6) Suzuki, K.; Ikari, K.; Imai, H. *J. Am. Chem. Soc.* **2004**, *126*(2), 462–463.
(7) Derrien, G.; Charnay, C.; Zajac, J.; Jones, D. J.; Roziere, J. *Chem. Commun.* **2008**, *27*, 3118–3120.
(8) Carroll, N. J.; Rathod, S. B.; Derbins, E.; Mendez, S.; Weitz, D. A.; Petsev, D. N. *Langmuir* **2008**, *24*(3), 658–661.
(9) Yamada, Y.; Yano, K. *Microporous Mesoporous Mater.* **2006**, *93* (1−3), 190–198.
(10) Nakamura, T.; Mizutani, M.; Nozaki, H.; Suzuki, N.; Yano, K. *J. Phys. Chem. C* **2007**, *111*(3), 1093–1100.
(11) Yano, K.; Fukushima, Y. *J. Mater. Chem.* **2004**, *14*(10), 1579–1584.
(12) Grün, M.; Kurganov, A. A.; Schacht, S.; Schüth, F.; Unger, K. K. *J. Chromatogr. A* **1996**, *740*(1), 1–9.
(13) Park, S.-E.; Kim, D. S.; Chang, J.-S.; Kim, W. Y. *Catal. Today* **1998**, *44*(1−4), 301–308.
(14) Fowler, C. E.; Khushalani, D.; Lebeau, B.; Mann, S. *Adv. Mater.* **2001**, *13*(9), 649–652.
(15) Cai, Q.; Luo, Z. S.; Pang, W. Q.; Fan, Y. W.; Chen, X. H.; Cui, F. Z. *Chem. Mater.* **2001**, *13*(2), 258–263.
(16) Rathousky, J.; Zukalova, M.; Kooyman, P. J.; Zukal, A. *Colloids Surf., A* **2004**, *241*(1−3), 81–86.
(17) Nooney, R. I.; Thirunavukkarasu, D.; Chen, Y. M.; Josephs, R.; Ostafin, A. E. *Chem. Mater.* **2002**, *14*(11), 4721–4728.
(18) Lin, H. P.; Tsai, C. P. *Chem. Lett.* **2003**, *32*(12), 1092–1093.
(19) Moller, K.; Kobler, J.; Bein, T. *Adv. Funct. Mater.* **2007**, *17*(4), 605–612.
(20) Moller, K.; Kobler, J.; Bein, T. *J. Mater. Chem.* **2007**, *17*(7), 624–631.
(21) Kobler, J.; Moller, K.; Bein, T. *Acs Nano* **2008**, *2*(4), 791–799.

between the inorganic species and the surfactant molecules during the self-assembly process, while the early stage of formation is still not clear due to lack of experimental data.

Herein, by a great deal of convincing experiments, we found that the uniform, monodisperse, and stable mesoporous silica nanoparticles can be prepared in mild synthesis conditions (pH 6−10), and the particle size can be controlled from 25 to 200 nm by varying synthesis parameters and adding suitable additive agents including alcohols, amine, inorganic bases, and inorganic salts. Additionally, the certain acid−base buffer capacity of the reaction mixture is essential for the formation of mesoporous silica nanoparticles in the TEOS−CTA^+ system. A reliable approach of in situ pH measurement of the synthesis system has been developed to investigate the formation process of mesoporous silica nanoparticles.

Experimental Section

Chemicals. Tetraethoxysilane (TEOS 98%), an aqueous solution of cetyltrimethylammonium chloride (CTAC, $C_{16}H_{33}N(CH_3)_3Cl$, 25 wt % in water), diethanolamine (DEA, $NH(CH_2CH_2OH)_2$), triethanolamine (TEA, $N(CH_2CH_2OH)_3$), ammonia (NH_3, 28 wt % aqueous solution), and other inorganic acids, bases, and salts were purchased from Beijing Chemical Works and used without further purification.

Preparation of Mesoporous Silica Nanoparticles. The mesoporous silica nanoparticles were prepared by a general method where TEOS was added into aqueous solution containing CTAC, ethanol, and some amount of additive agents such as inorganic salts, DEA, ammonia, or TEA. The following is a typical synthesis example: 6.4 mL of water (0.36 mol), 0.9 g of ethanol (0.015 mol), 1.04 g of a 25 wt % CTAC solution (0.786 mmol), and 0.02 g of DEA (0.19 mmol) were mixed and stirred in a water bath at 60 °C for 30 min. Then 0.73 mL of TEOS (3.25 mmol) was added into the mixture dropwise within 2 min under stirring. The solution turned white gradually. A further 2 h of stirring was necessary. Finally, the solution was cooled to room temperature.

Characterization. The morphologies and dimensions of the samples were revealed with a JEOL JSM-6700F field-emission scanning electron microscope (FE-SEM) and a JEOL JEM-3010 transmission electron microscope operating at 300 kV. Small-angle X-ray diffraction (XRD) patterns for the mesoporous silica nanoparticles were obtained on a Siemens D5005 diffractometer using Cu Kα radiation. The IR spectra were recorded with a Bruker IFS 66v/S FTIR spectrometer. The thermogravimetric and differential thermal analysis (TG-DTA) curves were recorded with a Perkin-Elmer Pyris Diamond TGA/DTA thermal analyzer at a temperature-increase rate of 10 °C min^{-1} under nitrogen. The adsorption−desorption isotherms of nitrogen were measured at 77 K using a Micrometeritics TriStar 3000 system. The pore size distributions were calculated from the adsorption branches of N_2 adsorption−desorption isotherms based on the BJH model. Dynamic light scattering (DLS) studies were carried out on a Malvern NanoZS zetasizer at room temperature. In situ pH of the reaction mixture was measured with a CH instruments 660C voltammetric analyzer by using directly a glass pH electrode.

Results and Discussion

For the synthesis of uniform mesoporous silica nanoparticles with controlled particle sizes, we used a number of additive agents to adjust the hydrolysis and condensation processes of silicon alkoxide. In fact, most additive agents with certain acid−base buffer capacity can supply OH^- directly or indirectly in the synthesis system. The OH^- acts as the basic catalyst for the sol−gel process of silica. A summary of experimental parameters and the corresponding abbreviations of products are shown in Table 1. The selection of additive agents and the evolution of our design are discussed in the following.

According to Bein's work, triethanolamine (TEA) acted as a complexing agent for silicate species and additionally as an encapsulator for mesoporous particles in the preparation of colloidal suspensions of nanometer-sized mesoporous silica.[19] TEA could limit the growth and aggregation of nanoparticles. We obtained almost the same result ($S_{T\text{-}60}$, ~80 nm, see Table 1 and Figure 1a) in our laboratory by a typical reaction condition as reported in Bein's paper.[19] The synthesis of mesoporous silica nanoparticles with TEA is repeatable and reliable.

The formation of colloidal particles with CTA^+ as template, just like normal MCM-41, should be a kinetic process involving a combination of sol−gel process of silica and self-assembly of silicate species with surfactant. The balance between hydrolysis and condensation of silica species in the presence of CTA^+ plays the key role in the synthesis. The chelating properties should not be the sole key factor for the formation of mesoporous silica nanoparticles. To explore the key factors for the synthesis of the mesoporous silica nanoparticles, we chose DEA which does not possess chelating properties to silica species instead of TEA to adjust the pH value of synthesis system. A high quality colloidal solution of particles with size of ~30 nm (see Figure 1b) was obtained easily from the DEA synthesis system.

The successful synthesis of nanoparticles in the DEA system did lead us to conclude that the chelating properties of TEA are not the sole key. These results encouraged us to consider that an additive agent as well as other synthesis parameters can control the right hydrolysis and condensation processes to form nanoparticles. The additive agent plays the key role in the synthesis. On the basis of this thought, all chemicals that are able to supply OH^- and have enough effects on the sol−gel process of silica can be used as additive agents. In the next example, ammonia was used. The synthesis results indicate that the additive agent ammonia can give uniform spherical nanoparticles (see Figure 1c). The product quality is similar to those in TEA and DEA systems.

It is worth mentioning that the amount of TEA can be varied within a wide range (from TEOS/TEA = 1:4 to 1:1). The change of TEOS/TEA resulted in the formation of different size nanoparticles from ~100 nm to ~50 nm as reported by Bein.[19] The effect of DEA or NH_3 on the formation of uniform nanoparticles is shown only in the range of TEOS/DEA = 1: 0.055 to 1:0.11 and TEOS/NH_3 about 1:0.09. We did not observe the obvious changes of nanoparticle size when DEA or NH_3 was used as additive agent. The reason may be the narrow adjustable change range. More DEA or NH_3 cannot give

Table 1. Synthesis, Experimental Parameters, and the Corresponding Abbreviations of Products in the Text[a]

sample[b]	additive agent	initial pH of synthesis system	temperature	reaction time	average diameter TEM	average diameter DLS
$S_{T\text{-}60}$	0.46 g of triethanolamine	10.0	60 °C	2 h	80 nm	
$S_{D\text{-}40}$	0.02 g of diethanolamine	9.6	40 °C	2 h	30 nm	60 nm
$S_{D\text{-}60}$	0.02 g of diethanolamine	9.6	60 °C	2 h	50 nm	
$S_{N\text{-}60}$	0.055 g of NH_3 solution (2.8 wt. %)	9.8	60 °C	2 h	60 nm	
$S_{100\text{-}60}$	0.5 g of solution of $Na_2B_4O_7$ (18.3 mmol/L)−NaOH (26.8 mmol/L)	10.0	60 °C	2 h	30 nm	58 nm
$S_{90\text{-}60}$	0.5 g of solution of $Na_2B_4O_7$ (25 mmol/L)−NaOH (1.77 mmol/L)	9.0	60 °C	2 h	30 nm	
$S_{85\text{-}60}$	0.5 g of solution of $Na_2B_4O_7$ (19.2 mmol/L)−HCl (23.3 mmol/L)	8.5	60 °C	2 h	45 nm	79 nm
$S_{80\text{-}60}$	0.5 g of solution of $Na_2B_4O_7$ (17.7 mmol/L)−HCl (29.1 mmol/L)	8.0	60 °C	2 h	45 nm	
$S_{75\text{-}60}$	0.5 g of solution of Na_2HPO_4 (168 mmol/L)−NaH_2PO_4 (32 mmol/L)	7.5	60 °C	3 h	65 nm	91 nm
$S_{70\text{-}60}$	0.5 g of solution of Na_2HPO_4 (122 mmol/L)−NaH_2PO_4 (78 mmol/L)	7.0	60 °C	3 h	75 nm	
$S_{60\text{-}60}$	0.5 g of solution of Na_2HPO_4 (24.6 mmol/L)−NaH_2PO_4 (175 mmol/L)	6.0	60 °C	5 h	85 nm	106 nm

[a] For each preparation, 0.73 g of TEOS, 1.04 g of CTAC (25%), and 0.9 g of ethanol were used. The ratio of main components TEOS/CTAC/H_2O/ethanol = 1:0.27:137:5.6. [b] The letters and numbers in the sample name stand for the additive agent used, initial pH of reaction mixtures, and reaction temperature. For example, T = triethanolamine, D = diethanolamine, and N = NH_3, $S_{100\text{-}-60}$ stands for the sample synthesized at 60 °C, and a buffer solution (pH = 10.0) was used as additive agent.

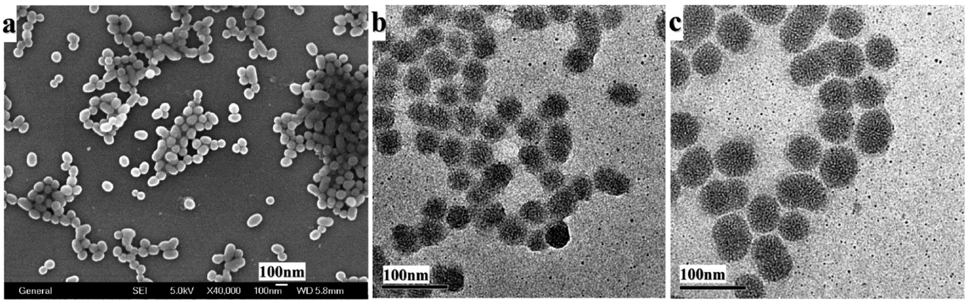

Figure 1. SEM and TEM images of the samples synthesized with different amines and ammonia: (a) $S_{T\text{-}60}$ with TEA (SEM), (b) $S_{D\text{-}40}$ with DEA (TEM), and (c) $S_{N\text{-}60}$ with NH_3 (TEM).

the spherical particles but elongated particles. The optimized amount of DEA or NH_3 is much lower than that of TEA.[19] The possible reason comes from their basic properties. Their pK_a values are on the order of NH_3 (9.2) > DEA (8.9) > TEA (7.8). Addition of a large quantity of TEA does not change the pH of the reaction mixture greatly, while a little amount of DEA or NH_3 can change the sol−gel process in our synthesis system due to their higher pK_a's.

The formation of mesostructural silica nanoparticles is a sol−gel process of silica in the presence of surfactant. The sol−gel process involving silicon alkoxides includes two main reactions, hydrolysis and condensation.[22,23] The pH of the reaction system can be an effective index of the sol−gel process of silica.[24] The pH−time curves encompass abundant information of the hydrolysis and condensation of the silicon alkoxide. We tried to measure in situ the pH of the synthesis systems of nanoparticles and to further understand the chemical process.

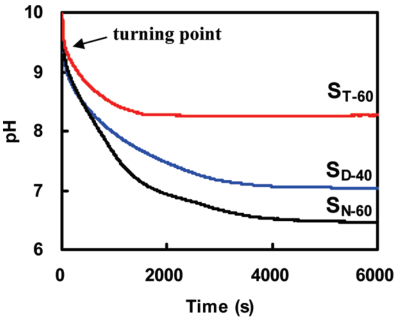

Figure 2. pH−time curves for reaction mixture of the samples: (a) $S_{T\text{-}60}$ with TEA, (b) $S_{D\text{-}40}$ with DEA, and (c) $S_{N\text{-}60}$ with NH_3.

Figure 2 shows the changes of pH for reactions with TEA, DEA, and NH_3 as additive agents. The pH value for the TEA system remains almost constant after 30 min, while the pH value decreases gradually for the DEA and NH_3 systems. The fast reaction for TEA system may result from the use of a large amount of TEA. Interestingly, the pH values of all syntheses decrease rapidly after the addition of TEOS, and two different reaction rates are

---

(22) Iler, R. K. *The Chemistry of Silica: Solubility, Polymerization, Colloid and Surface Properties and Biochemistry of Silica*; Wiley-Interscience: New York, 1979.

(23) Brinker, C. J.; Scherer, G. W. *Sol-Gel Science: The Physics and Chemistry of Sol-Gel Processing*; Academic Press: Boston, 1990.

(24) Nagao, D.; Osuzu, H.; Yamada, A.; Mine, E.; Kobayashi, Y.; Konno, M. *J. Colloid Interface Sci.* **2004**, *279*(1), 143–149.

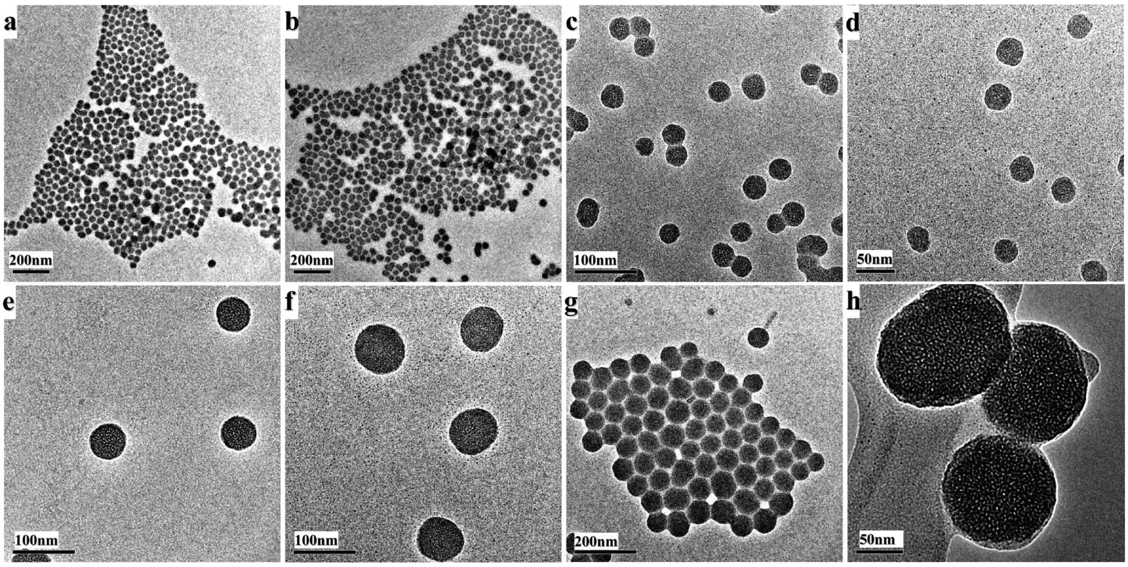

Figure 3. TEM images of the samples synthesized with different additive agents (different initial pH values): (a) S_{100-60}, (b) S_{90-60}, (c) S_{85-60}, (d) S_{80-60}, (e) S_{75-60}, (f) S_{70-60}, and (g and h) S_{60-60} (see Table 1 for the detailed synthesis parameters and particle size).

observed in the early stages of the reactions. The reaction solutions turned cloudy at the turning point of the pH decrease, which implied the existence of plenty of nanoparticles. The nanoparticles at this stage may be different from the final product. Further growth and structural optimizing may happen. Thus, combining with the uniform and monodisperse characteristics of these particles revealed by TEM and SEM (Figure 1), we can conclude that the formation of mesostructural nanoparticles follows the nucleation−growth mechanism. The nucleation of the nanoparticles may occur simultaneously just before the turning point of the pH decrease.

To understand the formation process of mesoporous silica nanoparticles and study the synthesis chemistry in a wide reaction condition (e.g., pH range), we introduced other kinds of additive agents into our synthesis system. To effectively control the hydrolysis and condensation processes of silicon alkoxide in the synthesis system, we considered following factors when we selected additive agents: (1) adjustable pH values from 6 to 10, (2) certain pH buffer capacities, (3) organic compounds that affect solution properties (e.g., polarity, solubility of reactants) or hydrolysis and condensation of silica (e.g., alcohol), and (4) extension to general inorganic base and salt.

We adjusted the initial pH value of the reaction mixture with different additive agents (inorganic buffer solutions; see Table 1). Our experimental results indicate that the initial pH value of the synthesis system is the main factor affecting the particle size of the product. The TEM images of as-synthesized samples show that the size of the particles increases from 30 to 85 nm with the decrease of the pH value from 10 to 6 (see Figure 3). The particles have the same size (~30 nm) when the initial pH values of synthesis system are above 9. All the particles are uniform and monodisperse spheres (see Figure 3) and contain disordered mesopores (see Figure 3h). All the samples in this paper have similar wormlike mesopores and arrangement of mesopores.

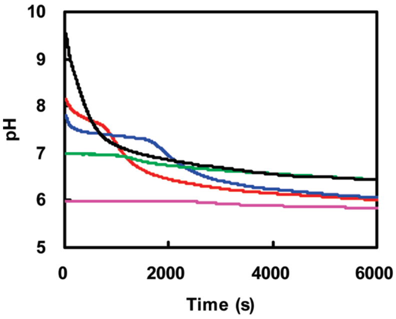

Figure 4. pH−time curves for the synthesis system of the samples: S_{100-60} (black line), S_{85-60} (red line), S_{80-60} (blue line), S_{70-60} (green line), and S_{60-60} (pink line) (see Table 1 for the detail synthesis parameters).

The formation of nanoparticles in our study follows the base catalyzed hydrolysis and condensation reactions of TEOS.[22,23] But the reaction rates are much faster than those of the classical sol−gel system without surfactant (e.g., TEOS + EtOH + H_2O + NH_3 system). The cationic surfactant molecules or micelles attract negative charged silica species, which concentrate silica species around micelles according to the formation mechanism for general mesoporous silica materials.[25]

Figure 4 shows the pH−time curves for the systems with different initial pH values. The pH curves for all samples have the same tendency. The curves for samples S_{85-60} and S_{80-60} (initial pH = 8.5 and 8.0, respectively) show very clear turning points and steps corresponding to the particle formation stages, while the pH value of the reaction system without surfactant CTAC decreases from 8.4 to 6.2 within 40 s and the hydrolysis of TEOS is not complete after 3 h reaction.

Here, we take the curve for S_{80-60} as an example to illuminate the change of pH in the formation process of mesoporous silica nanoparticles. First, the rapid pH

---

(25) Xu, R. R.; Pang, W. Q.; Yu, J. H.; Huo, Q. S.; Chen, J. S. *Chemistry of Zeolites and Related Porous Materials: Synthesis and Structure*; John Wiley & Sons: New York, 2007.

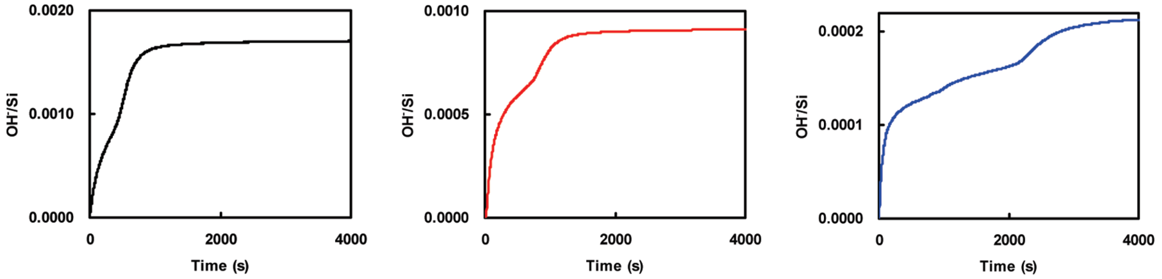

Figure 5. $[OH^-]/[Si]$−time curves for reaction mixture of the samples synthesized with different amounts of additive agent, solution of $Na_2B_4O_7$ (19.2 mmol/L)−HCl (23.3 mmol/L): S_{85-60a} (0.75 g of additive agent solution, black line), S_{85-60b} (0.5 g of additive agent solution, red line), and S_{85-60c} (0.25 g of additive agent solution, blue line).

decrease in the first few minutes is primarily attributed to the fast deprotonation of protonated silanols resulted from hydrolysis reaction. The hydrolysis rate of silicon alkoxides decreases after the initial rapid decrease of pH, which gives a plateau within the range of 300−1700 s in the curve for sample S_{80-60}. Then, another fast decrease of pH is observed, and the reaction solution turns cloudy because of the nucleation of nanoparticles occurring at this time. After that, pH decreases very slowly, which is corresponding to the growth of nanoparticles. Under our synthesis condition, hydrolysis and condensation reactions should occur simultaneously. We did not observe any remarkable pH increase during the whole measurement period.

As for the sample S_{85-60}, a calculation indicates that there are ~250 particles per cubic micrometer and the average distance between two particles is about 120 nm based on the silica density of particles 1.6 g cm^{-3} calculated from pore volume of nitrogen adsorption.

Figure 5 shows the $[OH^-]$ consuming curves calculated from pH changes for the system with the same initial pH value (pH = 8.5) but different amount of additive agent. The three curves in the figure have the same shape and clear steps. But with the reduction in the amount of additive agent in the mixtures, the reaction rates decrease gradually (i.e., reaction times increase).

The acid−base buffer capacity (supply OH^- capacity) of reactant mixture (please note the scale difference of *y* axes in Figure 5) affects the formation process of nanoparticles. The amount of OH^- released from the additive agent is far from sufficient for the hydrolysis of the entire TEOS. On the basis of the chemical analysis of silica concentration in dialysis solution of nanoparticles product via a membrane with cutoff 8−14k Da, 92% of TEOS forms nanoparticles after 3 h of reaction. The OH^- released from the condensation reaction must circulate through the formation of particles and act as a catalyst for the whole sol−gel process of silica.

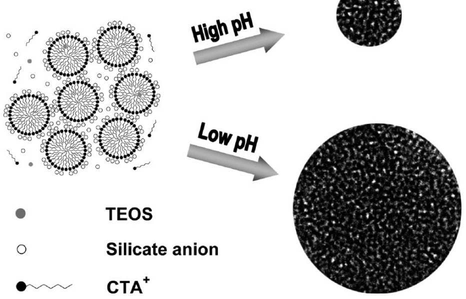

Figure 6. Scheme of the formation process of monodisperse mesoporous silica nanoparticles with different sizes.

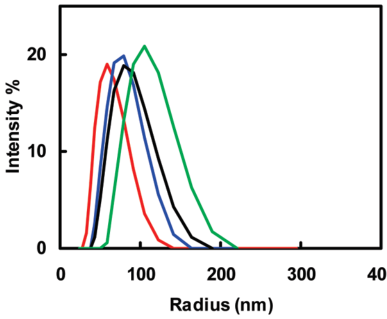

Figure 7. DLS measurements of samples synthesized with different additive agents: S_{100-60} (red line), S_{85-60} (blue line), S_{75-60} (black line), and S_{60-60} (green line) (see Table 1 for the detail synthesis parameters).

The descriptions of mesoporous silica (e.g., MCM-41 and MCM-48) formation mechanism reported in the literature[25−27] are mainly based on the solid product structure. The formation of nanoparticles is a simplified synthesis of mesoporous silica. The synthesis of nanoparticles is a short-time process and is relatively easy to study. Here, our experimental observations of the in situ pH measurement supply new evidence for the formation mechanism of MCM-41 reported.

The aggregation of micelles can be considered as a nucleus of a mesoporous silica nanoparticle. More micelles with silicates as counter-ions form around the nucleus or join the nucleus to form a nanoparticle. When the nanoparticle grows to a certain size, the growth will stop. The main reason is that the accumulation on silicate anions in a nanoparticle results in high net negative charge. When the net charge is high enough, the highly negative charged particle refuses to allow the new silicate anions to join this particle. Fewer silicate species are needed for high charge density silicates (small particles for the high pH cases), and more silicate species are needed for low charge density silicates (large particles for the low pH cases) to reach the maximum net charge of the particle (see Figure 6). As a consequence, the initial pH of the

---

(26) Firouzi, A.; Atef, F.; Oertli, A. G.; Stucky, G. D.; Chmelka, B. F. *J. Am. Chem. Soc.* **1997**, *119*(15), 3596–3610.

(27) Firouzi, A.; Kumar, D.; Bull, L.; Besier, T.; Sieger, P.; Huo, Q.; Walker, S.; Zasadzinski, J.; Glinka, C.; Nicol, J..; et al. *Science* **1995**, *267*(5201), 1138–1143.

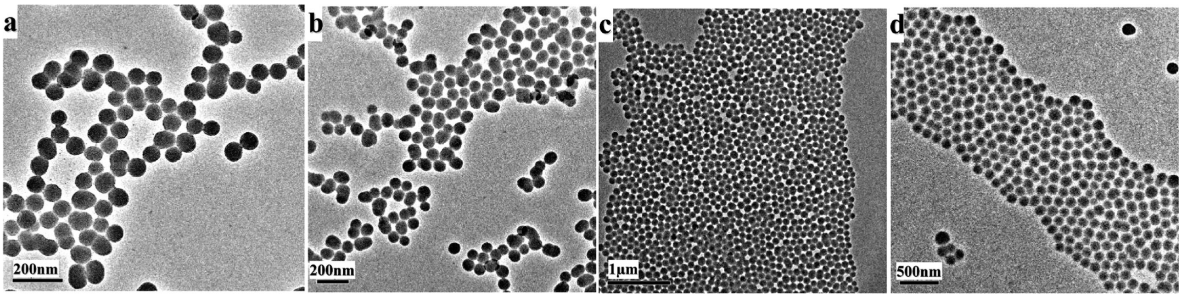

Figure 8. TEM images of the samples synthesized with different amounts of ethanol: (a) ethanol/TEOS = 6.8, particle size 75 nm, (b) ethanol/TEOS = 8, particle size 90 nm, (c) ethanol/TEOS = 10, particle size 130 nm, and (d) ethanol/TEOS = 11, particle size 155 nm.

synthesis system determines the product nanoparticle size. This process is responsible for the second rapid pH decrease for the samples S_{80-60} and S_{85-60}, and the growth of particles is relative to the following pH slow decrease.

According to the discussion above, larger particles will be prepared when the initial pH of the solution is lower. We used different $Na_2HPO_4-NaH_2PO_4$ solutions (initial pH = 7.5, 7.0, and 6.0) as OH^- sources. The products are monodisperse particles with mean diameters of 65 nm, 75 nm, and 85 nm, respectively (see Figure 3 and Table 1), which are highly consistent with our expectation. The DLS measurement (Figure 7) implies that the diameters of the samples S_{100-60}, S_{85-60}, S_{75-60}, and S_{60-60} are about 58 nm, 79 nm, 91 nm, and 106 nm, respectively.

Moreover, we discovered that under our reaction conditions (initial pH=6−10), the silicate species proceed via a base (OH^-)-catalyzed hydrolysis reaction. If both H^+ and OH^- had played the catalytic role, the reaction mixture would have contained the same amount of catalysts at pH = 6 and 8, and the particles would have had the same size. However, the dimension of S_{60-60} (initial pH 6, 85 nm) is obviously larger than that of S_{80-60} (initial pH 8.0, 45 nm) in our experiment.

According to the discussion above, other reactants and synthesis parameters which significantly affect hydrolysis and condensation of silica can determine the quality and size of nanoparticles. Ethanol was chosen and tested to control the hydrolysis and condensation of TEOS because ethanol plays a key role in the sol−gel process of silica.[22,23] In the DEA synthesis system, particles with various sizes (from 25 to 150 nm) can be obtained by varying the amount of ethanol from EtOH/TEOS = 5.6 to 11 (Figure 8). The formation of large particles results from the suppressing effect of ethanol on the hydrolysis of TEOS. Other alcohols such as propanol and ethylene glycol have the same effect, and propanol can give large particles up to ~200 nm.

We characterized our product mesoporous silica nanoparticles using different analytical techniques. The results show that the mesophase is ordered and the surfactant in the mesophase can be removed. In contrast to the multiple sharp peaks of ordered MCM-41 bulk materials, our samples only give one broad Bragg peak at low angles (2θ ~1.9°, see Figure 9). Commonly, XRD peaks become broadened or disappear with decreasing of particle size or disordering of mesostructure.

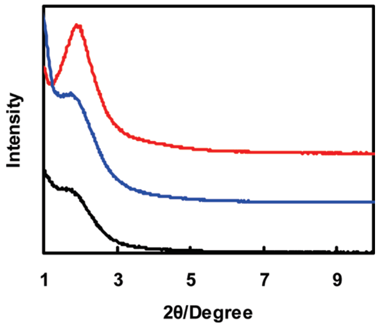

Figure 9. XRD patterns of different particle sized silica nanoparticles synthesized with different amounts of ethanol: 150 nm (red line), 90 nm (blue line), and 30 nm (black line).

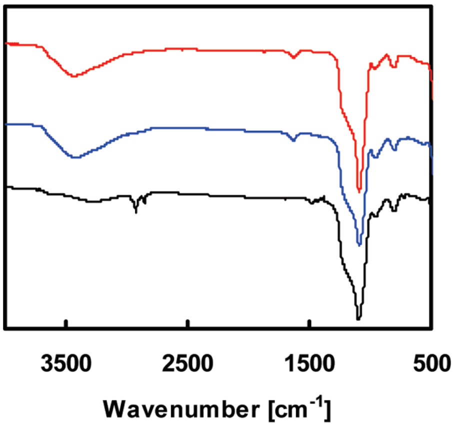

Figure 10. IR spectra of samples: as-made (black line), after extraction (blue line), and after calcination (red line).

The IR spectra of sample $S_{D\text{-}40}$ before and after extraction and calcination show that the C−H stretching vibrations between 2830 cm^{-1} and 2970 cm^{-1} and the C−H bending vibrations at 1470 cm^{-1} almost completely disappear after extraction and calcination (see Figure 10), which indicates that the templates are successfully removed after extraction with ethanol or calcination at high temperature. The water bending vibration at 1630 cm^{-1} is observed, which is attributed to the much more hydrophilic silanols on the silica surface after template removal.

The calcined sample exhibits high surface area, large pore volume, and narrow pore size distribution. For the nitrogen adsorption−desorption at 77 K, the calcined samples with different particle sizes (30, 90, and 150 nm) give the typical type IV isotherms with a hysteresis

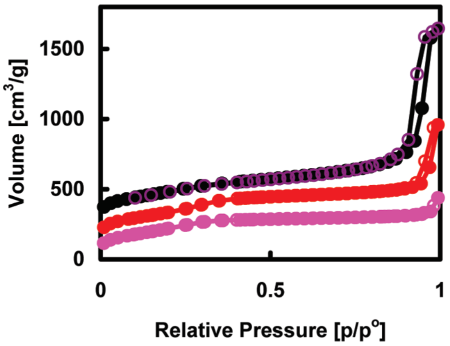

Figure 11. N_2 adsorption−desorption isotherm of different particle sized samples synthesized with different amounts of ethanol: 30 nm (black line), 90 nm (red line), and 150 nm (pink line). The isotherms are offset vertically by 100 cm^3 g^{-1} (for the 90 nm sample) and 250 cm^3 g^{-1} (for the 30 nm sample), respectively.

(see Figure 11). The BET surface areas are 851 m^2 g^{-1}, 852 m^2 g^{-1}, and 802 m^2 g^{-1}, respectively, and high pore volumes are 2.1 cm^3 g^{-1}, 1.4 cm^3 g^{-1}, and 0.8 cm^3 g^{-1}, respectively. All three samples have similar pore sizes (~2.1 nm) as determined with the BJH method based on the adsorption branch data. The small particle size is responsible for the textural porosity indicated by the hysteresis at high relative pressures. As the diameters of the particles decrease, the hystereses become more and more obvious.

Conclusion

In summary, uniform and monodisperse mesoporous silica nanoparticles have been prepared successfully in a moderate condition (initial pH = 6−10). The size of mesoporous silica nanoparticles could be controlled in a range of 25−200 nm by addition of different additive agents to adjust the hydrolysis and condensation of silica species

The in situ pH measurement of the synthesis system was used to investigate the formation process of mesoporous silica nanoparticles. The formation of mesoporous silica nanoparticles is a typical sol−gel process of silica in the presence of surfactant. The combination and balance of hydrolysis and condensation processes of silica species determine the formation of the nanoparticles. The size of the nanoparticles is mainly determined by hydrolysis of silica species (controlled by the initial pH of the synthesis system), and the nucleation of nanoparticles is determined by the condensation of silica species. High quality nanoparticles result from the homogeneous growth of simultaneous nucleation. The addition of additive agents with certain acid−base buffer capacity makes the above processes possible. The amphiphilic cationic surfactant makes above processes much easier and faster. The high reaction temperature (~60 °C) is necessary for the formation of nanoparticles.

The mesoporous silica nanoparticles are stable and can be used for many applications. In our laboratory, a number of experiments in catalyzing the cascade reaction and absorbing toxic anions such as CrO_4^{2-} by functionalized mesoporous silica nanoparticles are in progress.

Acknowledgment. This work was supported by the National Natural Science Foundation of China (20788101). The authors thank Xuejing Cao for assistance with the SEM measurements.